

SOLDIER VERTICAL MOBILITY SYSTEM: STABLE LOWER EXTREMITY EXOSKELETON

A Thesis
Presented to
The Academic Faculty

by

Quincey D. Lowery

In Partial Fulfillment
of the Requirements for the Degree
Master of Science in the
School of Mechanical Engineering

Georgia Institute of Technology
May 2018

COPYRIGHT © 2018 BY QUINCEY D. LOWERY

SOLDIER VERTICAL MOBILITY SYSTEM: STABLE LOWER EXTREMITY EXOSKELETON

Approved by:

Dr. Jun Ueda, Advisor
School of Mechanical Engineering
Georgia Institute of Technology

Dr. Aaron Young
School of Mechanical Engineering
Georgia Institute of Technology

Courtland Bivens
Georgia Tech Research Institute (GTRI)
Georgia Institute of Technology

Date Approved: April 27th, 2018

Table of Contents

List of Figures.....	iv
Chapter 1	1
1.1 Introduction.....	1
1.2 Motivation.....	2
1.3 Research Objectives.....	2
Chapter 2	4
2.1 Overview of Chapter.....	4
2.2 Exoskeleton History	4
2.3 Landing Injury Studies.....	6
Chapter 3	8
3.1 Problem Statement.....	8
3.2 Protective Suits.....	9
Chapter 4	13
4.1 Parallel & Serial Connection	13
4.2 Proof of Concept	23
4.3 The Device.....	25
4.4 System Modeling	28
Chapter 5	31
5.1 Method	32
5.2 Experimental Setup	34
5.3 Results	37
5.4 Discussion.....	43
Chapter 6	46
Conclusion & Future Work	46
Appendix.....	48
References.....	50

List of Figures

Figure 1 Body protection: Whole body covered (a); Ideal protection w/ viscoelastic material (b)	10
Figure 2 Possible injury when landing: Muscle and tendon (a); Bone and cartilage (b)	11
Figure 3 Joint and bone protection: translational series and parallel impedance (a); muscle and rotational parallel impedance (b).....	14
Figure 4 1-DOF four element.....	16
Figure 5 Protection of muscles and tendons viscoelastic model	17
Figure 6 Protection of bones and cartilages viscoelastic model	17
Figure 7 Parallel viscoelasticity: parallel damping (a); parallel spring (b); parallel rigidity (c).....	19
Figure 8 Serial viscoelasticity: Serial rigidity (a); Serial elasticity (b); Serial damping (c)	22
Figure 9 Exoskeleton: Prototype (a); Schematic (b)	24
Figure 10 Viscoelastic comparison	25
Figure 11 Impact sim 800 N/m	29
Figure 12 Impact sim 1200 N/m	30
Figure 13 Impact sim 1000 N/m	30
Figure 14 1DOF sim model	31
Figure 15 Muscle: Vastus medialis oblique [9]	32
Figure 16 Muscle: Tibialis anterior [9]	33
Figure 17 Muscle: Soleus [9]	34
Figure 18 EMG: VMO	35
Figure 19 EMG: SOL.....	36
Figure 20 EMG: Tibialis anterior.....	36
Figure 21 VMO 0.5ft	39
Figure 22 SOL 0.5ft	39
Figure 23 TA 0.5ft	40
Figure 24 VMO 1.0ft	40
Figure 25 SOL 1.0ft	41
Figure 26 TA 1.0ft	41
Figure 27 VMO 1.5ft	42
Figure 28 SOL 1.5ft	42
Figure 29 TA 1.5ft	43

Chapter 1

1.1 Introduction

The call to action was brought upon by Georgia Tech Research Institute (GTRI) and JetPack Aviation. The mission is to create a functioning wearable device that allows enhanced vertical mobility as well as resistance to pilot landing. The Soldier Vertical Mobility System (SVMS) is to provide soldiers with the ability to function normally in movement with some assistance. JetPack Aviation's vertical take-off and landing device is to be paired with subsystems to ensure safety for the pilot. The systems are expected to provide reliability, assist survivability, using mechanical designs and other human factors.

JetPack Aviation has designed and manufactured the first personal flying device [18]. The true need for this has yet to be established, however there is a need to enhance the devices safety features.

In flight the pilot is tightly secured in through harnesses that run through the jetpack. The upper half of the body (waist up) is secured, while the lower half of the body is loosely suspended in air. Upon landing the pilot typically feathers the throttle to ensure a safe landing. The term "safe" means minimal damage to joints in the lower half of the body. As the pilot feathers the landing he/she has to reach for the ground with one foot. Thus far, the pilot lands on one leg and the other follows. The reason for this feathered throttle landing is to safely land on the surface without providing an injury to the body [18]. Future plans call for the pilot to be able to land two conjointly and become mobile instantly.

1.2 Motivation

With any new innovation safety becomes the primary concern. In cars and airplanes, the seatbelt was designed to secure the passenger in motion, motorbike riders wear helmets. These items serve as protection against injuries [8]. The military is in need of new technology that can enhance soldier protection during pursuit of their missions.

In protective devices the initial question is understanding what body parts need protecting the most. This research is based off simulations and tests conducted for a jetpack pilot. The focus is to protect and minimize damage that could be done to those joints in the leg. The damage can be inflicted by excessive ground reaction forces or improper landing posture. A look into the joint analysis of the exoskeleton device will provide information on how the system operates. Data collected from electromyography tests gives insight into how muscle protection differs from wearing a protective device and not wearing the device. Electromyography (EMG) will record muscle activity displaying how the various regions react upon surface contact. With an interest in reducing the energy experienced on the human body, EMG will assist in finding ways to achieve this.

1.3 Research Objectives

Throughout this study, muscle activity data was collected for insight on protecting joints and muscles in the legs. The use of this information is to reach the conclusion that the use of an exoskeleton device protects the human body when coming in contact with the ground. The aim is to discover if the conceptual design for the viscoelastic protective device is effective and translates into protecting the human body. A viscoelastic model works in a manner of materials under mechanical constraints and to use this knowledge to predict its behavior of the biological materials [19]. Given the need for a wearable soldier

vertical mobility system (SVMS), a design with constructed parts is required before experimental testing. The constructed parts consist of utilizing spring-damper systems to protect limbs. The exoskeleton design will primarily focus on protection of the patella, hip and ankle. These specific joints were selected as means of emphasis considering the effects in the legs upon ground reaction contact.

The SVMS device was expected to prevent hyperextension and protect joints and muscles from outside forces created through impact with ground surface. One objective was to measure and analyze muscle activities in selected muscles (vastus medialis oblique muscle, soleus muscle, and tibialis anterior muscle). Muscle activity was measured using electromyography sensors to determine how these muscles perform with and without the exoskeleton. Comparing EMG results is expected to assist with conclusions about the effectiveness of the viscoelastic protective device. The comparative data includes determining what effects the exoskeleton has on the body and what effects not wearing the exoskeleton does. Ultimately the plan is ensure the exoskeleton is protecting the limbs and reducing ground impact.

Chapter 2

2.1 Overview of Chapter

The state of this project is novel; so, there is not any prior research on this problem. However, there is some prior research related to protective devices. Critical to this project is the need for a device that has the ability to enhance mobility while providing shock absorption assistance. Most of the prior work discovered focuses separately on the uses of robotic exoskeletons or examining joints and muscles in the legs. The collection of reviewed works was produced by several universities and research institutes [3][5]. This chapter presents a summary of historical work on exoskeletons and a review of landing studies.

2.2 Exoskeleton History

Development of robotic exoskeletons began in the mid-1900s. Developed to mimic human motion and enhancing human strength to enable heavy object lifting [1]. Similar to exoskeletons of modern day, the focus has been on providing humans with the ability to hold heavy payloads. In 1965, General Electric began development of the Hardiman. The Hardiman was one of the earliest models of strength enhancing exoskeletons. Though technology was not very advanced [1], studies were conducted to make breakthroughs in engineering.

The University of Wisconsin-Madison was able to develop an assistive walking device that has assisted locomotion [1]. This system can sustain the weight of the human wearer and limits the user to unidirectional motion. The lack of complexity in the design limited the range of motion in the exoskeleton. Towards the beginning of the 21st century

exoskeleton development increased and entered the market for gait rehabilitation. People with spinal cord or stroke injuries can use these devices to assist with walking and motion rehabilitation. Gait rehabilitation devices, such as Lokomat [20], take control of the patient's legs to recreate muscle memory. The computer controls the pace for walking strengthening the leg muscles. Besides the medical industry, exoskeletons are being used to enhance the mobility and strength of military soldiers.

Within recent years there have been numerous advances to enhance the strength and mobility of soldiers. Modern technology has led to the creation and development of Lockheed Martin's Human Universal Load Carrier (HULC) which allows users to support a heavy payload on their back. Funding from the American Defense Advanced Research Projects Agency (DARPA) and Raytheon [1] have been developing a robotic suit since 2000 with the intent of creating a "super soldier".

At the University of California, Berkeley, the Human Engineering & Robotics Laboratory developed what is known as the Berkeley Lower Extremity Exoskeleton (BLEEX). This concept in some ways resembles the jetpack and subsystem connection. The BLEEX design was developed to enhance endurance and strength on the human user. The device is a load transferring system that can sustain a payload of 70lbs [3]. Any excess weight is transferred to the pilot. BLEEX design mimics that of a human leg to allow the pilot to have a near perfect walking motion. The Berkeley lab focused on creating knee, ankle, and hip joints that matched the human body. For our exoskeletal design we also wanted to follow that same mindset. Similar to BLEEX we wanted to ensure the pilot had functional motion as if the device was not being worn.

BLEEX designers state “the primary goal of a lower-extremity exoskeleton is locomotion [3]” meaning that lateral and vertical motion are important. Clinical gait analysis performed to determine typical walking patterns and joint analysis on the human body. Considering that each person has a variation in gait, the system was scaled to a specified standard. For JetPack Aviation, there is a designated sizing for the pilot. Having a standard is beneficial to formulating data and getting expected results. Results for the angle, torque and power of the ankle, hip and knee are based on the motion of heel strike and toe-off. The results show that the toe-off creates similar patterns in the ankle and knee angles. The greatest amount of power to move the body is in the hip which naturally would seem plausible. Experimental results show that the ankle averaged a power rating of 100W [3], faring higher than the other joints. Although the current exoskeleton which is described later in this paper is not controlled, the amount of power can be useful for further iterations.

2.3 Landing Injury Studies

In the military landing injuries can occur through parachuting. Paratroopers experience injuries through improper landing practices, increase in winds, excessive equipment, time of day, or method of transportation [13]. Preventive measures that have been taken to prevent the risk of ankle injuries during landing consist of using ankle braces. According to Knapik *et. al* the use of an ankle brace [13] has produced fewer ankle injuries amongst soldiers. Studies have shown that of 23,031 jumps taken, 16.9% of them resulted in ankle sprains or ankle fractures [7][17]. These types of injuries can be prevented through proper protection and landing techniques. The result of ankle fracture and sprains can potentially lead to chronic disorders.

Other injuries that can occur through parachuting include head and knee injuries. Concussions and head trauma come from anatomical motion with excessive ground reaction

forces. Ground reaction forces indicate the intensity of stress the body is subjected to on contact [16].

Paratroopers landing practices have resulted in numerous injuries over the years. The effects of these jumps have resulted in ankle injuries. The effects from these studies can be used in understanding how to limit the risk of injury in the ankle for a jet pack pilot. Utilizing the information regarding paratroopers will further benefit the use of a SVMS.

Chapter 3

3.1 Problem Statement

Jet Pack aviation has introduced a call to order to integrate the developed VMS with the pilot of the Vertical Take-off & Landing (VTOL) device [18]. Currently, the pilot has limited protection while in flight and is attached to a current VMS to create a soft landing upon touchdown. This system being the jetpack, developed for application in the areas of search and rescue, autonomous supply delivery, first responders, law enforcement, medical delivery and retrieval. Limited protection can result in damage towards the joints, muscles and bones given the immense weight of the system [11].

Currently, research displays limited information on protective exoskeletons efficiency. As mentioned earlier, conventional exoskeletons enhance human strength through the use of power actuators and other powered sources to guide the system. Body protection is sometimes overlooked when considering the bilateral nature between the interaction of the exoskeleton, human body and environment. Understanding the coupling dynamics of the human body and exoskeleton assists with placement of design features such as dampers and actuators.

Higher injury risks occur during hard landings. Steele *et. al.* discusses the injury risk factors from paratroopers in their high-impact landing. Stated in this research was that 30-60% of parachuting injuries result in damage to the ankle [7]. To prevent damage to sensitive regions a landing technique was developed to protect body from musculoskeletal injuries. To reduce the amount of injuries occurred through a hard landing, a wearable

mobility system in junction to the VTOL device will benefit the pilot. Preferably the device should provide mobility while walking and running in addition to shock absorption upon contact [2]. The wearable exoskeleton will absorb the forces that would generally be received by the body. According to Ueda *et al.*, [11] key functions of such an exoskeleton are 1) to protect the operator's bones and joints by mitigating landing shock with increased weight and 2) to provide a certain level of mobility for performing missions after landing. In theory the use of the lower extremity exoskeleton creates a soft landing for the joints.

3.2 Protective Suits

In falling capacities, the human body can be considered a fragile object that must be protected. Attaching viscoelastic materials to the body will allow these parts to deform to absorb the shock. Ideally, immersing the human body in soft materials would create the highest case for shock absorption. An example of this is labeled in the Figure 1a. Overall protection of the body will minimize the chances of joint and bone injury. The soft materials act as a casing for the human body limiting reaction motions that occur upon impact.

Figure 1a displays a landing where the body is completely covered in soft material. This scenario portrays an instance where the body is completely protected and engulfed in soft covering. This type of protection does not explicitly prevent the body from injury because the landing is not being absorbed. Ideally the use of viscoelastic material inside of the soft material would benefit overall protection. This method of protection illustrated in Figure 1b provides all-around protection for the body. This protection can absorb the shock experienced through the body by the application of the viscoelastic material.

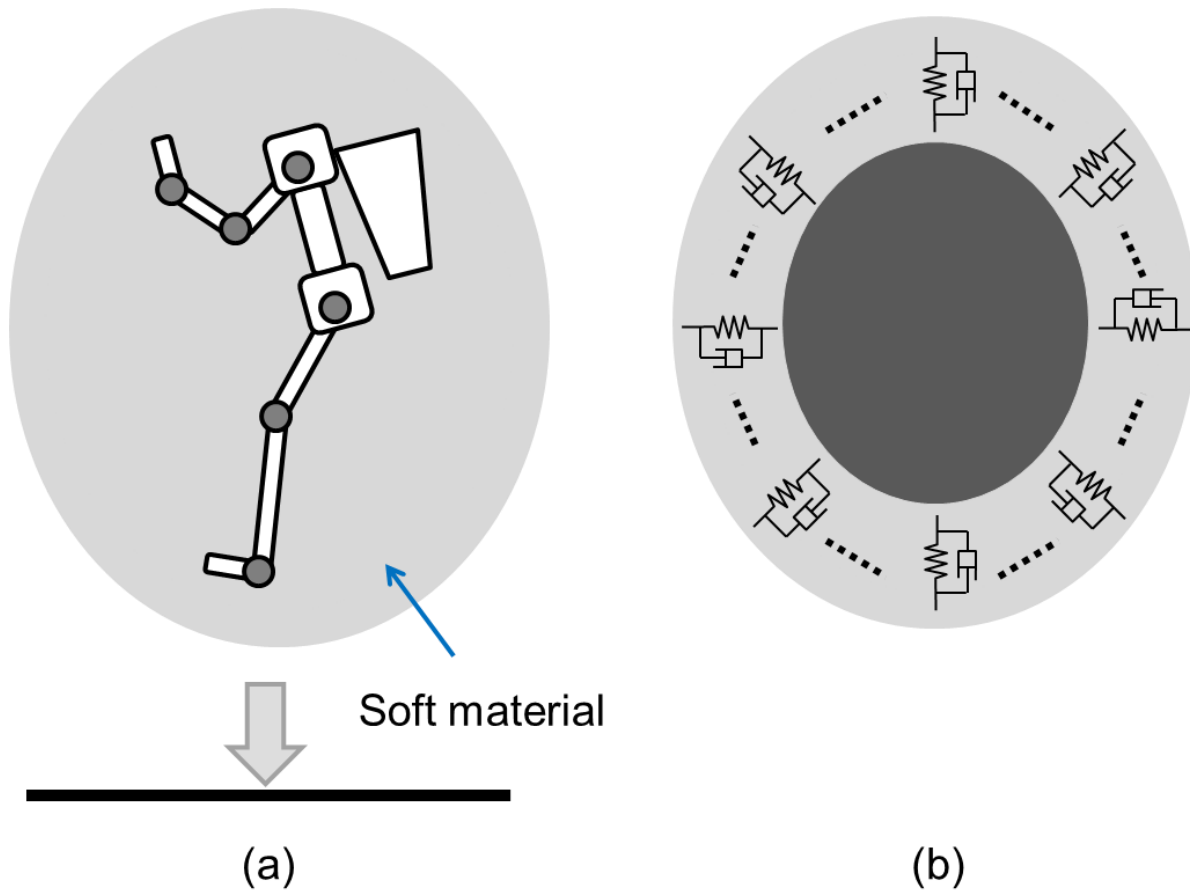


Figure 1 Body protection: Whole body covered (a); Ideal protection w/ viscoelastic material (b)

Muscles and tendons that are elongated beyond resting position on impact put the human musculoskeletal at risk of being damage. Prevention of this motion is imperative to sustaining intactness of limbs. Potential landing varying variations that can occur upon landing that cause bodily injuries are orthogonal positioning and parallel positioning. Parallel movement of limbs is a result of muscle and tendon injures created from excessive joint movements in the admissible motion space.

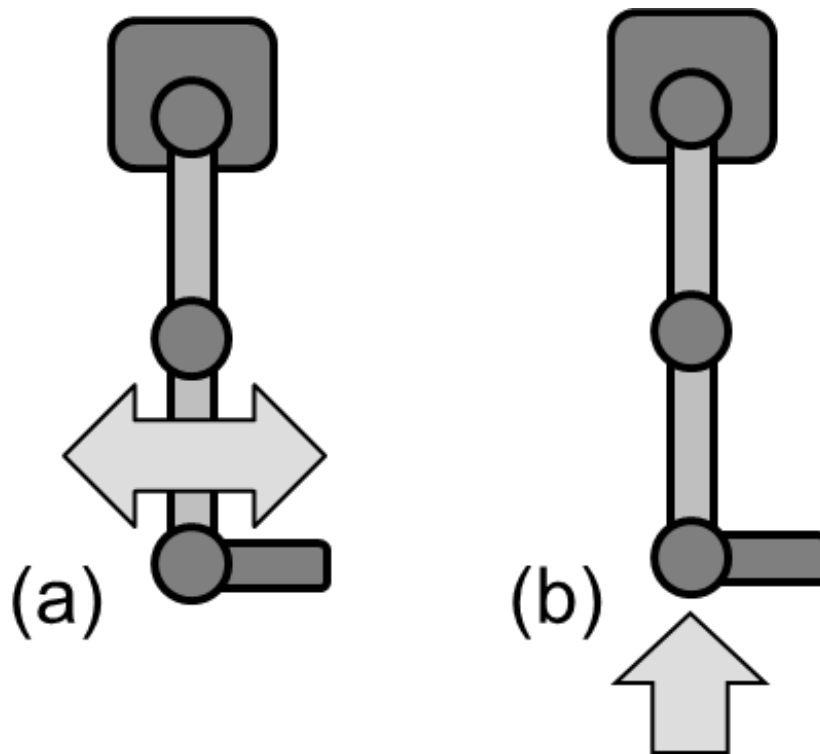


Figure 2 Possible injury when landing: Muscle and tendon (a); Bone and cartilage (b)

Figure 2a illustrates injury towards muscle and tendons based on the directional motion space. Lack of shock absorption potentially will result in the limbs exceeding their designated motion range. Movements that cause the limbs to exceed range space will damage the muscle and tendons.

Figure 2b illustrates a situation where bone and cartilage damage occur from excessive pressure in the translational direction on the limb. Excessive compression is a result of immense pressure received on the limbs. This pressure creates damage to bones and cartilage. The limb becomes constrained against natural extension. Compression in the

limbs crushes bones and cartilage. The amount of damage done in this direction depends upon the amount of external forces received. A greater amount of external forces received on the body increases the likelihood of injury to the limbs.

Chapter 4

4.1 Parallel & Serial Connection

This chapter will begin to introduce the multi-element viscoelastic models that inspire the work for body protection. Based on the discussions in the previous chapter about bone and cartilage injuries, the concept of a linear parallel and linear series connection would seem beneficial. The primary goal is to successfully protect and secure the limbs upon receiving external forces. As mentioned, to reduce the damage done on the body, a functional source needs to reduce the force experienced by the limbs. To prevent joints from exceeding anatomical range [11][12] connecting shock absorbing components.

External forces can create a variation of stresses on the bones and cartilage. Instantaneous and steady state mechanical stresses may create damage to the bones and cartilage [6]. The magnitude of instantaneous stresses generally exceed those of steady state stresses. Solving this issue involves dampening the instantaneous stress through application of serial impedance connected to the limb. Steady-state stresses need proper distribution that can be done by introducing a parallel connected impedance to the limb as shown in Figure 3a. From this schematic it is apparent that the translational forces that are applied onto the body are absorbed by the linear impedances. This concept will be reviewed again when examining the design of the exoskeleton.

Reverting back to the previous chapter where the pattern for muscle and tendon injuries are characterized in Figure 3a. Protection for muscle and tendons is done by introducing viscoelastic elements to be placed parallel to the joints. The viscoelastic elements operate in a manner that individually protect muscle regions of location. A

structural shell is placed to protect the thigh and shank areas. These shells are essentially bounded together to prevent rotation outside of expected range. The concept mimics general knee supports requiring prior engineering knowledge to properly distribute pressure between skin and shells.

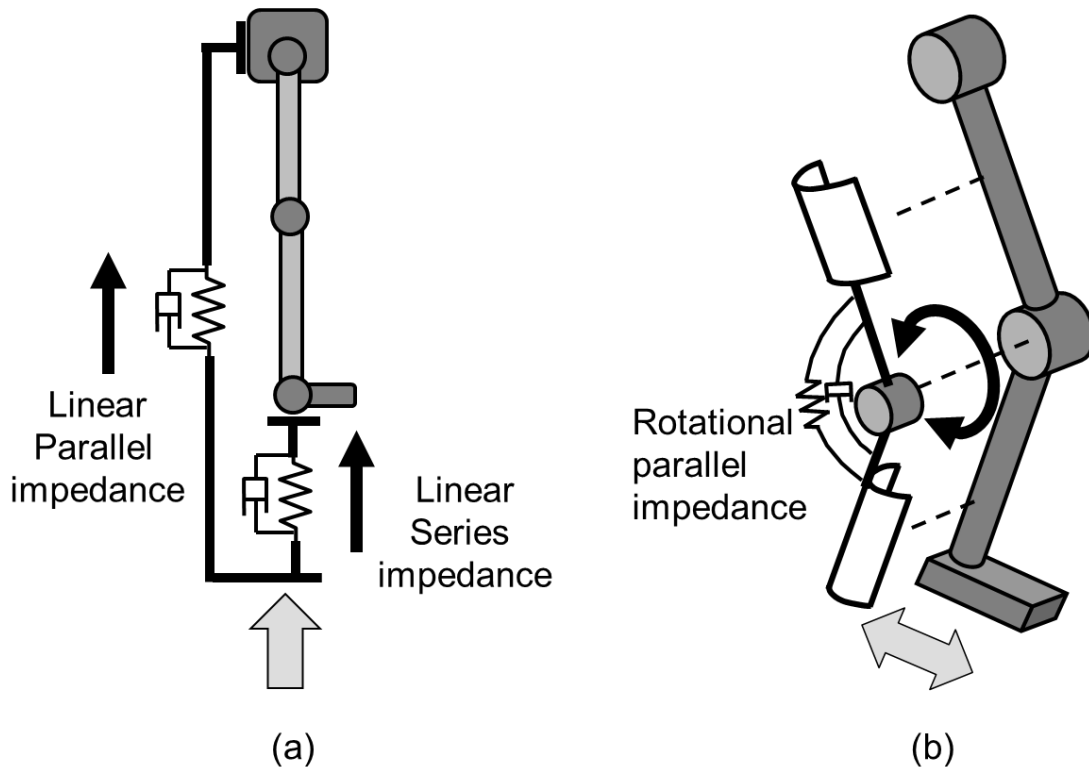


Figure 3 Joint and bone protection: translational series and parallel impedance (a); muscle and rotational parallel impedance (b)

The model labeled in Figure 3b is the fundamental model of viscoelastic elements protecting the joints. There are current devices that utilize this concept at higher level where rotational motion is controlled by a power source. This proves beneficial considering the device has a faster response to react and protect the muscles and tendons.

4.2 Rheology of Viscoelastic Representation

Models used to describe rheology of viscoelastic mechanical models include Maxwell, Kelvin-Voight and Zener [4]. In physiology and biomechanics the Hill model is commonly used to model muscle contraction. Throughout this section viscoelastic models are used to characterize the concepts described in earlier sections involving parallel and serial connections. The structures contain a cluster of elements connected in series and parallel. Models will display similarities to the Hill muscle as well as representation of an input-output relationship of an amplified piezoelectric actuator. Figures below are used to relate the joint and limb protection concepts with viscoelastic blocks. The multi-element linear viscoelastic model in Figure 4 can represent the shock absorbing dynamics of the ideal system.

The four element viscoelastic in the Figure 4 is an oversimplified model for the concept of bodily protection with a serial and parallel connection. Illustrated in this Figure is a human limb that is represented as a spring-damper system and force element that acts as the muscle. In the human limb section of the diagram displacement between the far left base and the elemental point is defined by x_h . Spring constant and damping coefficient are k_h and b_h respectively. An active resistance force f_m is placed to constitute the force the muscle generates. Viscoelastic serial connection 1 has a spring constant of k_{s1} and a damping coefficient of b_{s1} . Also connected to the human limb is another viscoelastic system with a parallel connection to the human limb. The elements in this subsystem are k_p and b_p for the spring constant and damping coefficient. The displacement between the first serial-parallel connection and the second serial connection is x_f . The final viscoelastic element connected to the serial-parallel connection has spring constant and damping

coefficient of k_{s2} , b_{s2} . The displacement between the third viscoelastic system and the environment is x_e , which receives a force f_e .

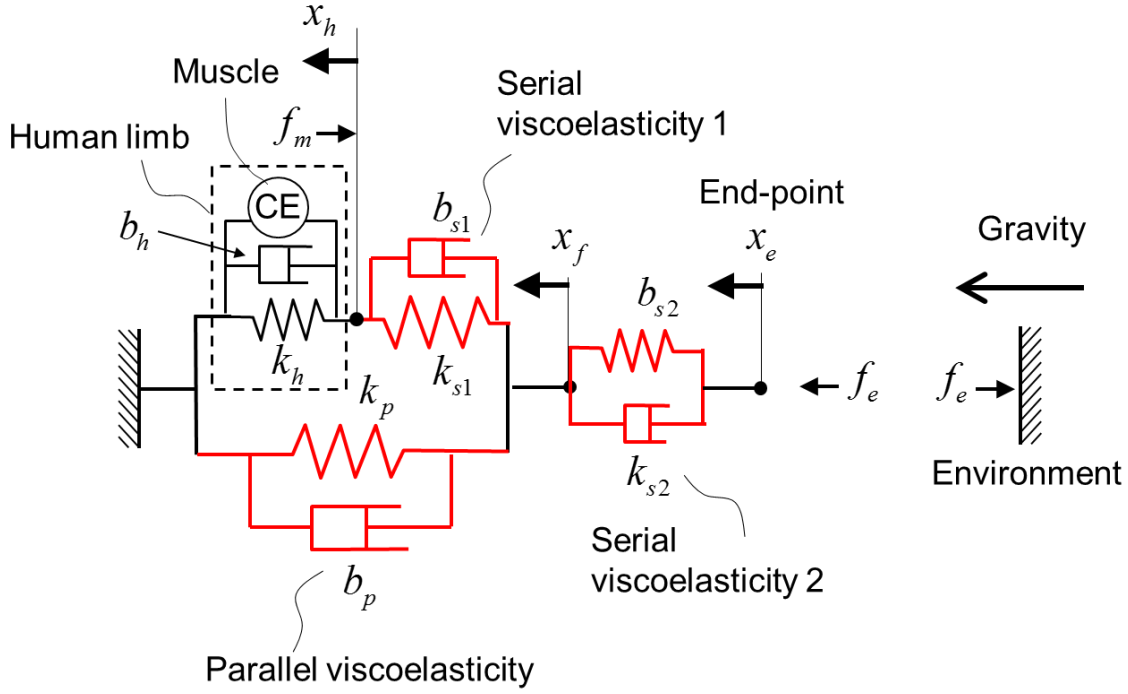


Figure 4 1-DOF four element

From Figure 4 the following equations are derived to the balance the forces throughout the viscoelastic elements. The shock force that human limb receives is characterized by represented equation (4).

$$f_m + k_h x_h + b_h \dot{x}_h = k_{s1}(x_f - x_h) + b_{s1}(\dot{x}_f - \dot{x}_h) \quad (1)$$

$$k_{s1}(x_f - x_h) + b_{s1}(\dot{x}_f - \dot{x}_h) + k_p x_f + b_p \dot{x}_f = k_{s2}(x_e - x_f) + b_{s2}(\dot{x}_e - \dot{x}_f) \quad (2)$$

$$f_e = k_{s2}(x_e - x_f) + b_{s2}(\dot{x}_e - \dot{x}_f) \quad (3)$$

$$f_h = k_h x_h + b_h \dot{x}_h \quad (4)$$

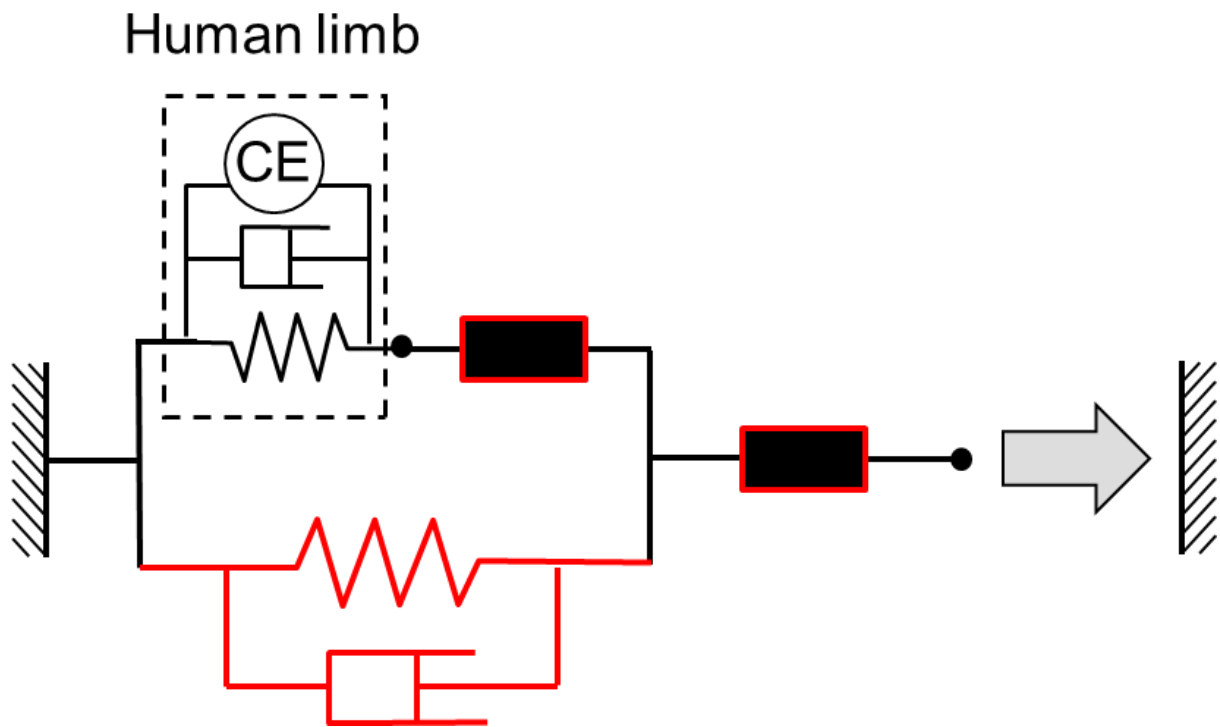


Figure 5 Protection of muscles and tendons viscoelastic model

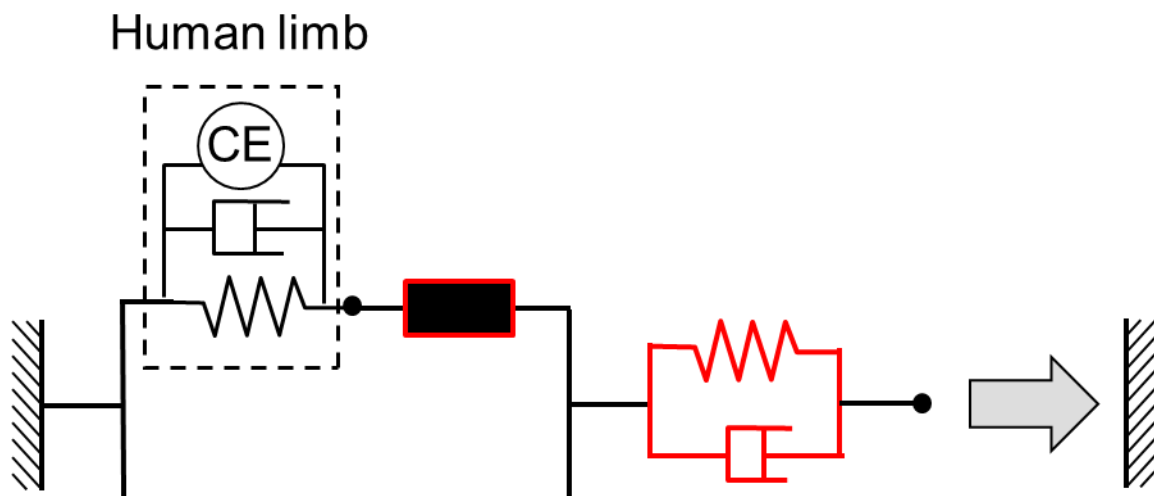


Figure 6 Protection of bones and cartilages viscoelastic model

The four element viscoelastic model can be modified in a manner that represents a simplified version of body protection. Subjecting the human limb to specific patterns of shock absorption similar to those outlined in the previous section, generates the following illustrations. Figure 5 is a representation of Figure 3b where the rigid members are the shells used to protect the muscles for rotational motion. The rigid members replacing the original viscoelastic blocks contain spring constant of $k_{s1}, k_{s2} \rightarrow \infty$ and damping coefficient of $b_{s1}, b_{s2} = 0$. The parallel impedance is represented from the parallel viscoelasticity block onto the human limb.

A look into the translational motion characterized in Figure 3a is represented by the viscoelastic model in Figure 6. This model has removed the serial-parallel viscoelastic system that was connected to the human limb block in Figure 4. In exchange a rigid member replaces to show protection of bones and cartilages. The serial viscoelastic element

that remains connected to the subsystem to the right operates as the shock absorption mechanism at the bottom of Figure 3a.

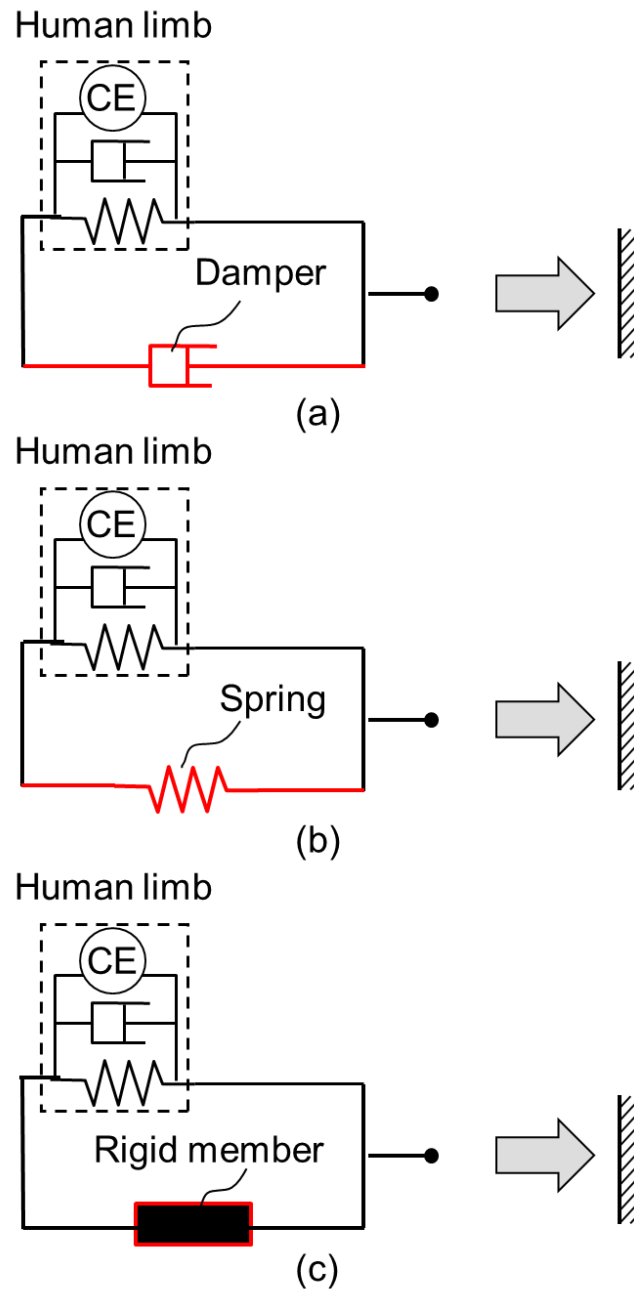


Figure 7 Parallel viscoelasticity: parallel damping (a); parallel spring (b); parallel rigidity (c)

Going forth simple cases of viscoelasticity will be discussed, cases involving solely parallel viscoelasticity and then solely serial viscoelasticity. In parallel viscoelasticity the objective is to limit the range of motion of the human joint. The following illustrations will explain how parallel viscoelasticity is able to accomplish this.

The varying impedance types illustrated in the above Figures defines k_h as a combined stiffness of the muscles and tendons. b_h is the contributing viscosity of the joint. The human limb block is a representation of the joint of interest, *ie*: the hip, ankle, or knee. Referring to the previously mentioned statement of parallel viscoelasticity limiting the range of motion, Figures 7a and 7b describe this by the use of a damper or spring. Use of a damper does not directly limit the range of motion, however larger instantaneous joint velocities increase the viscosity during shock. By doing so, the effect of induced shock limits the motion. The damper slows the motion of the joints and tendons upon impact protecting them against damage and injury.

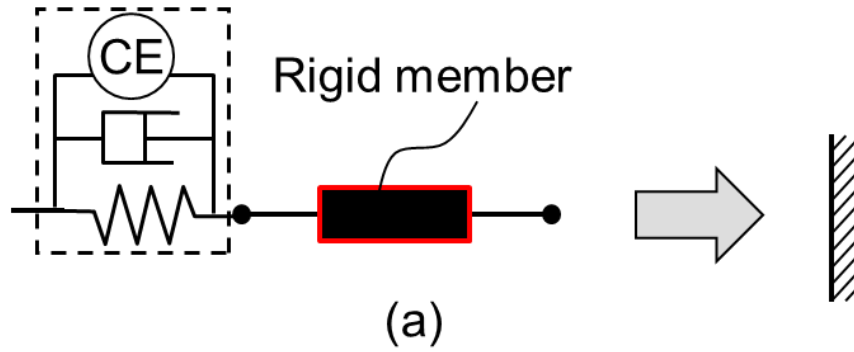
On the other hand when a spring is placed in parallel with the human body, the result is a direct limitation in the range of motion. Also, the spring experiences some of the direct loads that are transmitted to the limb. This dispersion of forces in turn would reduce the risk of injury. To effectively utilize the parallel spring model introducing a clutch mechanism is valid. This application will reduce the issues with mobility from the protective device.

Ideally for joint protection the joint stiffness is $k_p \rightarrow \infty$. In the case of parallel rigidity as seen in Figure 7c, the protection device receives all the external load, meaning

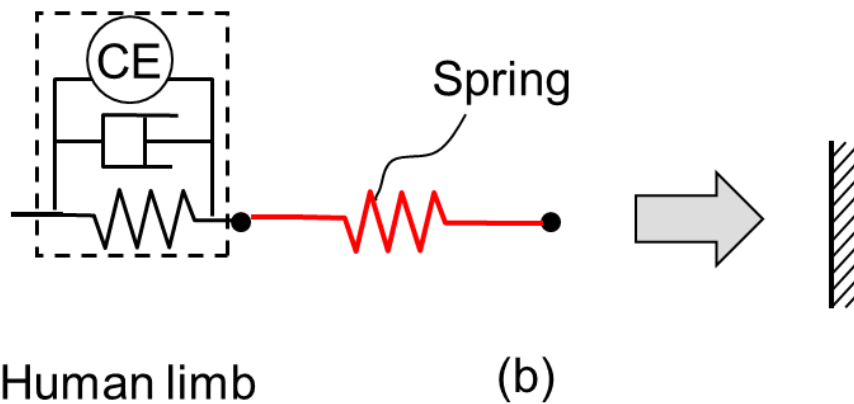
the limb is completely protected. Though the limb may be protected from external forces, it is important that the human limb does not exceed its anatomical range.

In serial impedance types the human limb block represents a combination of bone(s) and its cartilage(s). Series viscoelastic materials experience a higher spring stiffness k_h than its parallel viscoelasticity counterparts. The primary functionality of series viscoelasticity is to reduce large peak stress. Below the illustrations will show how this can be achieved with the placement of damping and spring parameters.

Human limb



Human limb



Human limb

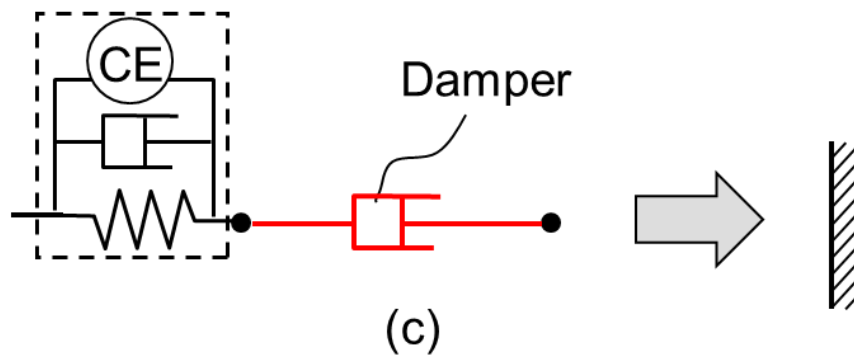


Figure 8 Serial viscoelasticity: Serial rigidity (a); Serial elasticity (b); Serial damping (c)

Figure 8a with the rigid member included in series contains no protection, thus resulting in the limb receiving direct forces. An unprotected limb increases the peak stress in the bone and raises the risk of injury to bone and cartilage. Reducing the peak stress in bone requires applying an elastic spring or damper. Elasticity in series is not favorable considering the spring component does not dissipate any energy after impact. Introducing an elastic component similar to Figure 8b will simply store the energy received from impact. This concept may be counter intuitive since it is not creating a soft landing for the user. However, applying a damping component in series seen in Figure 8c will dissipate energy from impact. Since a practical structure that is placed under the foot needs to have a certain level of stiffness to support the entire weight, a recommended design would be to combine a damper with high viscosity and a spring with relatively low stiffness [11].

4.2 Proof of Concept

Based on what was discussed in the previous section, for the specified VMS discussed in this section, a shock absorber should naturally be connected in series. This component is designed to mitigate shock experienced towards the bones and joints. Decreasing the risk of injury involves applying shock absorbers in parallel to the knee and ankle joint. This connection will satisfy the injury pattern described in Figure 4. Below is the wearable prototype designed and fabricated as proof of concept. This 2 DOF device contains parallel viscosity to the flexion of the knee joint. Plantar flexion and dorsiflexion are introduced to the ankle joint. Figure 9a represents the manufactured exoskeleton prototype that was fabricated from the schematic of Figure 9b.

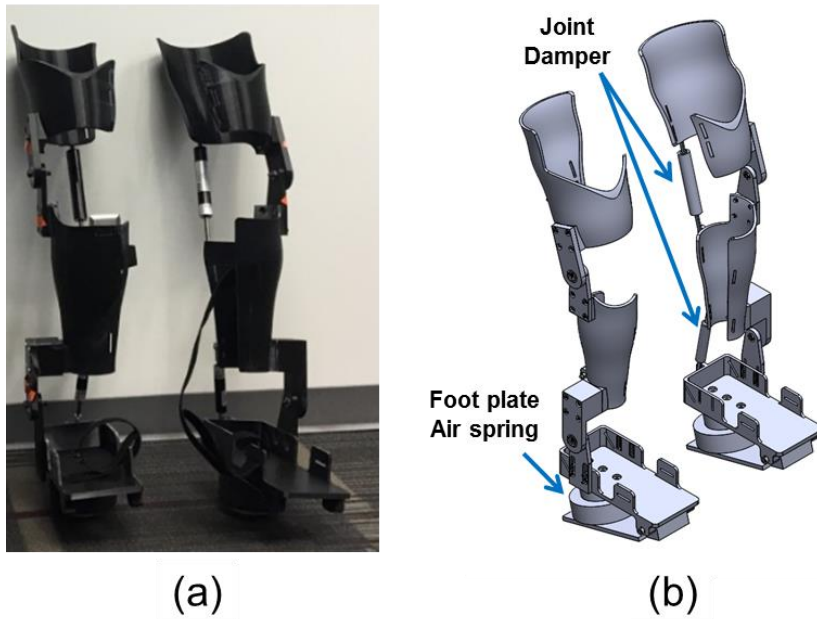


Figure 9 Exoskeleton: Prototype (a); Schematic (b)

The following Figure 10 illustrates the four element viscoelastic model and the corresponding components in the prototype. The human limb (thigh and shank) are secured inside the shells. Each limb is connected in parallel to the joint damping limiters. The limbs are in a serial connection with the foot of the wearer, where the shoe acts in a spring manner. The final serial viscoelastic block contains the shock absorber that is under the foot. This component is placed strategically to dissipate forces experienced upon impact and assist with reducing the risk of injury.

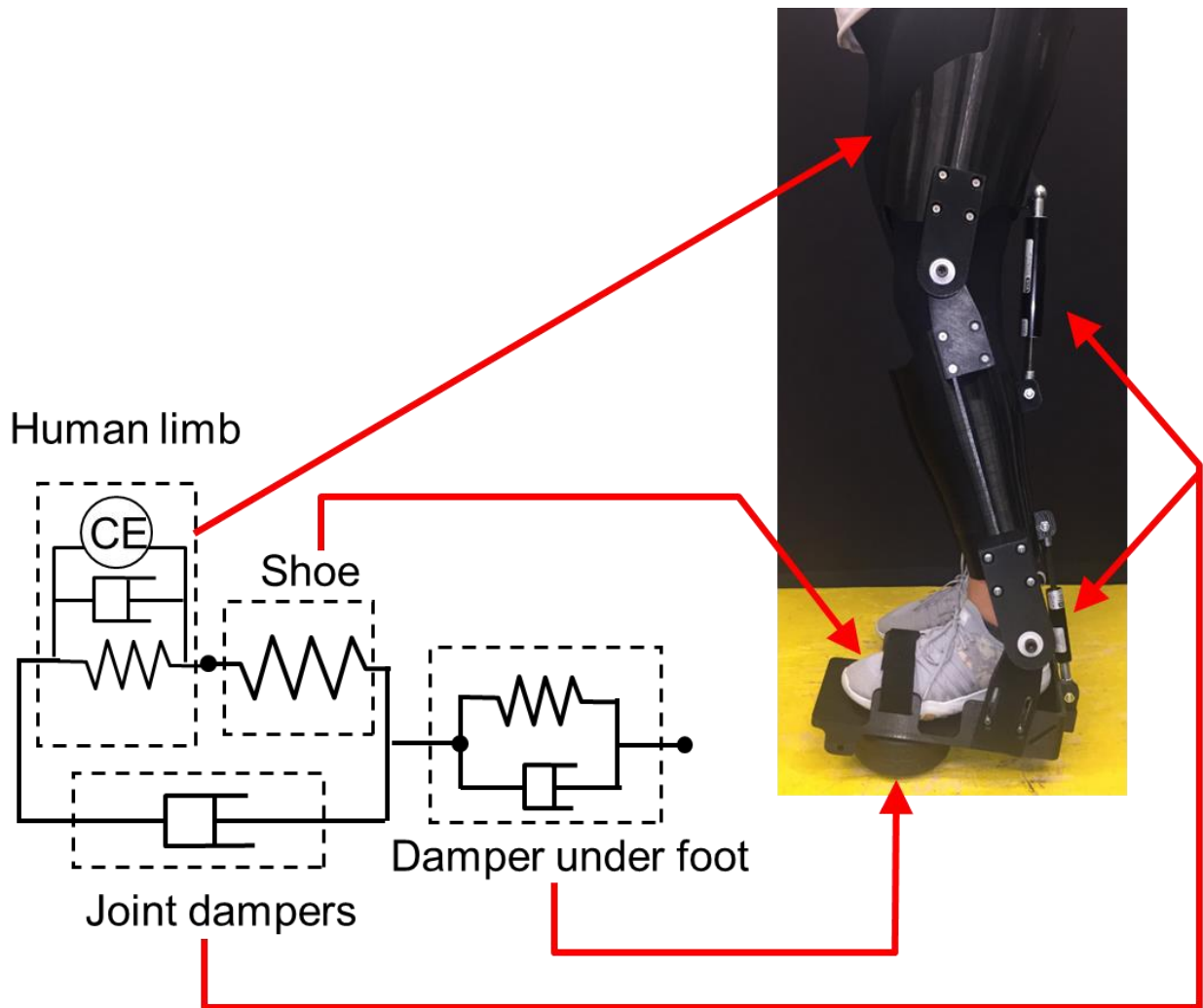


Figure 10 Viscoelastic comparison

4.3 The Device

The exoskeleton device was modeled with the intentions to fit the standard sized JetPack Aviation pilot. Sizing of the pilot can be found in Appendix, sizing of the pilot based on the given anthropometry chart. Pilot dimensions were transferred into SolidWorks to develop the alpha prototype of the exoskeleton. The model was scaled almost true to the dimensions of the pilot. The thigh is design in a manner to secure the hamstring and not prohibit the motion in the quadriceps. Providing enough room for the patella to be exposed

allowing for regular leg extension. Range of motion in the upper region is constrained by the limiter directly connected to the back of hamstring to the calf. Connection of the limiter was strategically placed based on sizing to allow the wearer to be fully extended in concession with the limiter.

Shank design allows for full insertion of the lower leg. Enough space was provided for the calf to have mild room between the muscle and the device. This was to ensure that the muscle was not constricted. Shank connection similar to the thigh connection has limiters attached. The bottom portion of the top limiter is connected to the top of the shank connection. Lower level of the shank contains the lower speed limiter which runs into the hind of the foot holder. Allotted area in this region gives motion to the ankle.

Limiters prevent the system from over rotating. Without the limiters the system can cause the legs to flex pass a 90 degree sitting angle. This is to ensure the body does not buckle upon initial contact with the ground. The lower limiters act as control between the ankle and foot. At the base of the exoskeleton lies an air tire that dampens the load on initial contact. On impact the tire is the first to come in contact with a surface and is placed at the front of the foot for typical landing body motion. Positioning the tire here is important because it mimics how the body would react in a situation without the exoskeleton. Throughout experimentation this was observed when watching the subjects land. This type of impact will settle the legs.

The exoskeleton design provides a range of motion to the knee joint of ± 28 degrees. In the ankle joint 0-45 degrees (plantar flexion) and 0-21 degrees (dorsiflexion). These ranges prevent the joints from hyper extension and over rotating. The overall purpose of

this device is to protect the joints and bone cartilage. The goal is to reduce and minimize damage to these regions so the body remains intact. Protection focuses on securing joints as well as bone cartilage.

Knee and ankle joints are protected inside the system and granted rotation. Rotational range is not to exceed anatomical motion of the joints. The knee region is designed similar to that of a knee brace. This allows the knee to breath and move in accordance to its several degrees of freedom. The knee rotates in the flexion (extension) direction.

Unlike most exoskeletons that contain some form of control actuator, this current design does not. The conceptual background behind this design was discussed in previous sections to provide an understanding as to why this is the case. From the concept modeling explained how the system operates in a serial & parallel connection for joint protection.

The viscoelastic system contains multi-element spring damper connection that operates in serial and parallel. Multi-element models are described to represent viscoelastic models in rheology. The deformation of the exoskeleton device is dependent about the ground reaction force and the parameters set by the adjustable limiters and dampers. Adjustable connections provide varying outcomes that can stiffen or loosen the linkages of the wearable device. Connections that are loose will not protection the limbs sufficiently creating damage in the joints. However, system with a higher stiffness will prevent fluid rotation of joints and will increase muscle activation upon impact.

Viscoelastic properties consist of the system deforming in accordance with the force reverted from the ground through the body. The exerted forces are intensified based on

parameters set on the system. Dampening limitations and stroke range create a varying deformation in the viscoelastic system. Improper deformation can lead to damage in the joints and other ligaments. To prevent improper deformation the pilot is to be situated in a manner that allows them to land in a manner that creates the maximum shock absorption. This can take place when the foot pressure tire experiences maximal stroke when contact takes place.

4.4 System Modeling

The viscoelastic system of the exoskeleton is characterized as a serial and parallel connection shown in Figure 9. What is examined is the breakdown of each of the components and how they are connected in relation to this. The wearable device is designed to absorb majority of ground reaction forces experienced when landing. Absorbing or limiting high ground reaction forces is important in this study. Reducing these forces limits the magnitude of instantaneous energy on the body. The three Figures (11-13) display force-time graph at varying spring constant values (800 N/m, 1000 N/m and 1200 N/m) and a constant damping coefficient of 500. Figure 14 illustrates a 1-DOF model that is used to simulate the outcomes from shown in Figures 11-13. The model applies spring and damper systems to each body element to reduce the external forces experienced by them.

What is important about this graph is that it illustrates the force response in the various regions after impact. In Figures 11-13 the greatest amount of force is experienced on the foot. Being that the foot makes the initial contact with the ground and is bearing the weight of the torso, shank, and thigh this would be the case.

Ideally the goal is to increase the time it takes to reach peak force. Once the maximal force has been achieved the body can gradually return to a steady-state. Increasing the time to achieve peak reaction force, reduces the amount of compression applied to the joints and muscles at one instant.

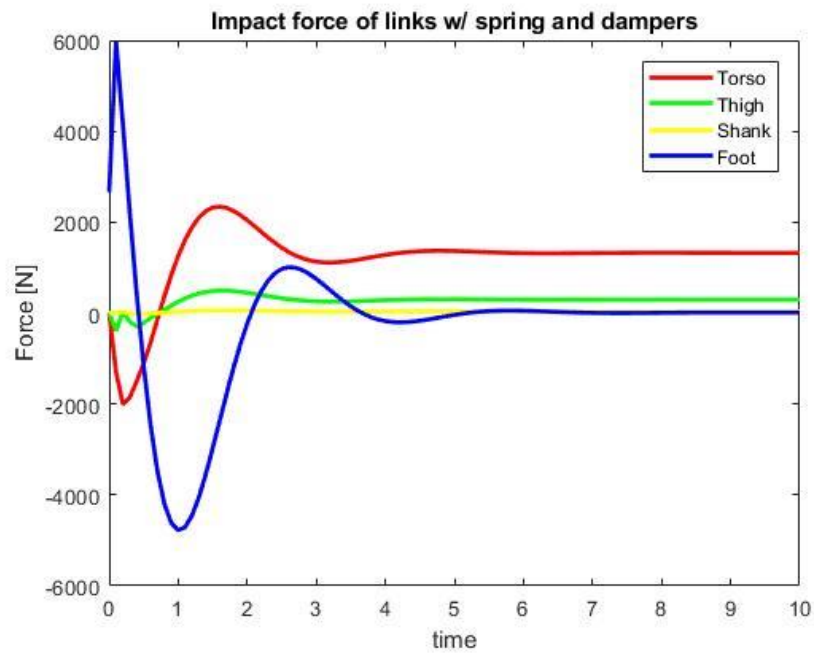


Figure 11 Impact sim 800 N/m

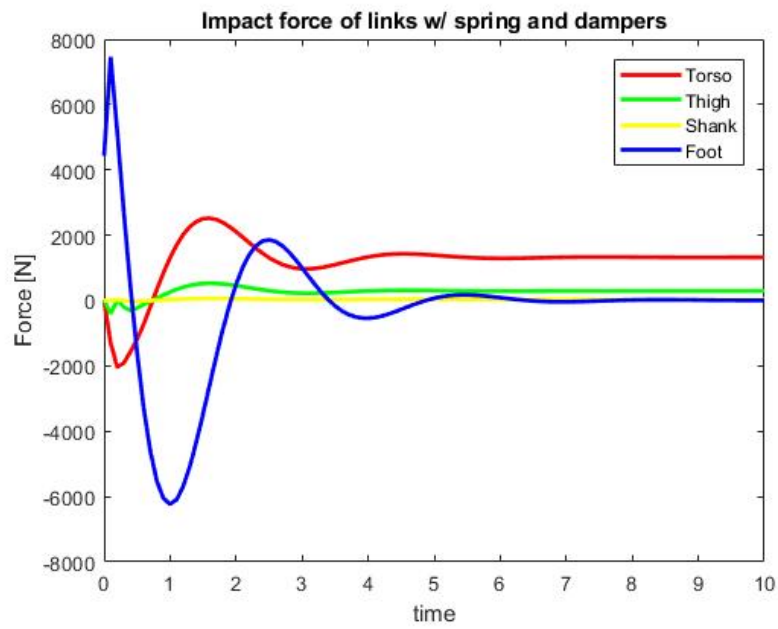


Figure 13 Impact sim 1000 N/m

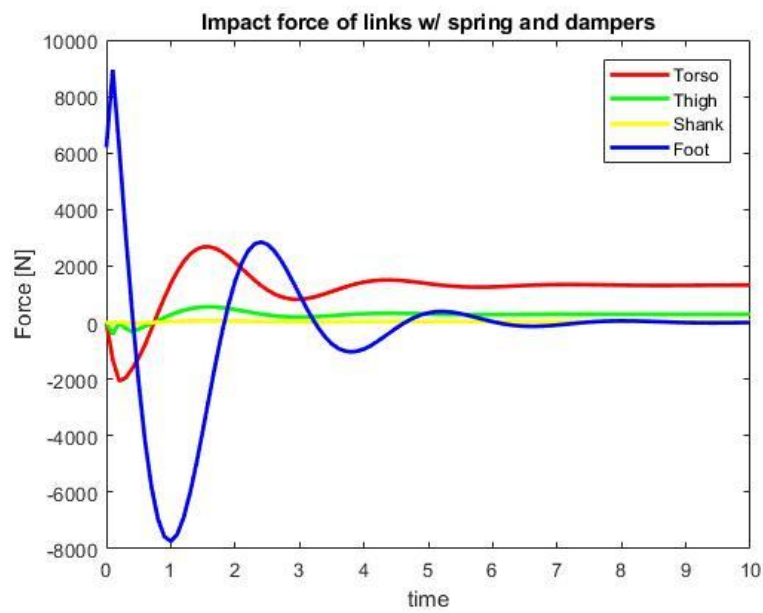


Figure 12 Impact sim 1200 N/m

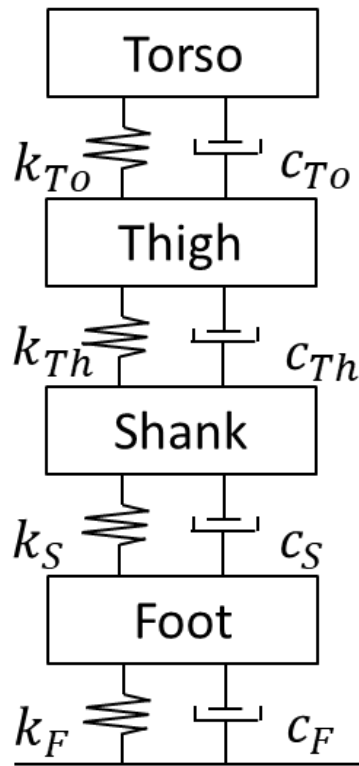


Figure 14 1DOF sim model

Chapter 5

5.1 Method

Experiments were performed following Protocol H17101 approved by the Georgia Institute of Technology Institutional Review Board (IRB). Ten volunteers on campus were recruited to perform the experiment utilizing the exoskeleton. Volunteer's data is Mean (SD); Age 22.1 years (0.99), Height 172.72 cm (9.8), and Weight 76.11 kg (11.77). Subjects did not have any current injuries or decencies in leg muscles and joints.



Figure 15 Muscle: Vastus medialis oblique [9]

Measured muscles included vastus medialis oblique muscle (VMO), soleus muscle, and tibialis anterior muscle. VMO muscle represents one of the four major muscles that make up the quadriceps. This muscle is a strong contributor to running, jumping, and other basic movements. VMO muscle is critical to stabilizing the knee, a weak VMO muscle can result in knee pain or even injuries.

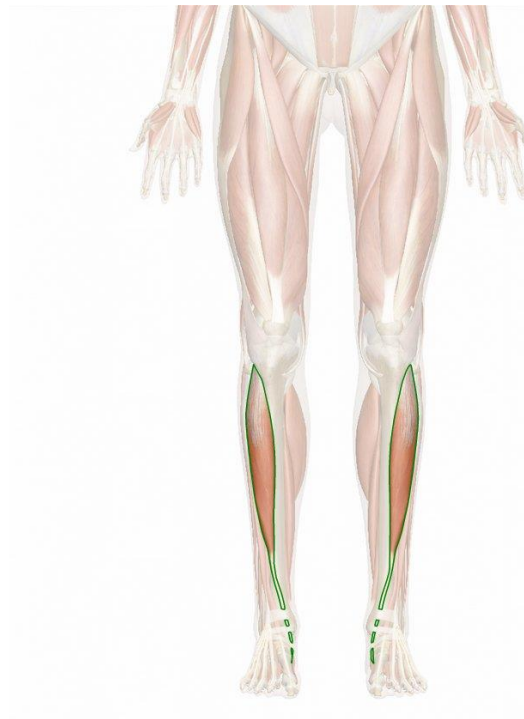


Figure 16 Muscle: Tibialis anterior [9]

Largest muscle present in the shank is the tibialis anterior muscle. Tibialis anterior muscle functions as a dorsiflexor of the foot by pulling the top, or dorsum, of the foot towards the shin. Providing slight inversion motion of pulling the plantar of the foot towards the body's midline [10], this motion assist with balancing the body on the foot during locomotion and while standing.



Figure 17 Muscle: Soleus [9]

Soleus (SOL) is located on the back of the lower leg and originates at the posterior aspect of the fibular head and the medial border of the tibial shaft. Primary function of the muscle is pushing off the ground when walking, soleus is vital in everyday mobile functions. It also helps maintain posture which prevents the body from falling forward.

5.2 Experimental Setup

Landing experiment involves the use of prototype exoskeleton to determine how muscles react when impacted by external surface force. Subjects were asked to perform a series of landings at the varying heights of 0.5ft, 1ft and 1.5ft. All subjects were required to be secured in a harness while performing the series of landings. During the landing process, subjects were instructed to have normal landing posture. Normal landing posture

consist of controlled two foot landing where the subject made contact with the ground on the balls of their feet. Also note that a normal landing posture required subjects to contain a slight flexion in the knee.

Devices include EMG sensors attached to the illustrated muscles in Figures 10(a-c).



Figure 18 EMG: VMO



Figure 20 EMG: Tibialis anterior



Figure 19 EMG: SOL

5.3 Results

What is to be solved in these series of tests is to prove that the design concept can protect the joints better than when compared to without the system. Going forward we will examine the effects how the legs muscles react while wearing the device and at a controlled state with no protection. Data was constructed through a process of using EMG to analyze muscle activity in the selected muscles of the leg. The collected data was filtered using a Butterworth low-pass filter to remove high frequency noise. All the EMG was normalized against each muscles maximal voluntary contraction (MVC). The following results display the comparison of not wearing the device to wearing the exoskeleton.

Reflected below represents the statistical results from the data collected from the subjects. The data characterizes a comparison of the subjects wearing the exoskeleton to not wearing the exoskeleton. The magnitude of this data is determined from ratio of the average value at that time stamp compared to the overall MVC value. Data from the VMO muscle illustrates that its peak muscle activity without the exoskeleton is 43.2% at 0.5ft, 40.9% at 1ft, and 65.8% at 1.5ft. Results from VMO were larger than those of SOL muscle and tibialis anterior muscle. Peak results for the SOL muscle without the exoskeleton are 30% at 0.5ft, 28.3% at 1.0ft and 38.4% at 1.5ft. The TA muscle contains max MVC% at 18.4% at 0.5ft, 16.6% at 1.0ft, and 65.8% at 1.5ft.

Experimental data is displaying the change in muscle activity. Expected results will determine if wearable device is dampening the amount of muscle activity in the respective regions. This scenario however, will not explicitly state that the exoskeleton is functioning

for full joint protection. The experiment focuses on understanding how muscles will react upon contact with the ground surface. Noticed through all the subjects was that their VMO muscle experienced the greatest amount of activity when compared to the SOL and tibialis anterior muscle. VMO muscle is larger than the other two muscles which does play into effect that amount of voltage received through the electrodes. The soleus muscle experiences the least amount of activity based on the positioning of the air cushion under the foot. The landing motion of the wearer does not fully excite the soleus muscle during the landing phase. User applies primary pressure on the front of their foot. The diagrams display each individual muscle's average comparison over the given time interval. Using T-test statistics, the error bars were generated throughout. The error bars characterize the range of between all the subjects.

What is expected to be seen from these bar graphs is a declining trend of the data over time with a magnitude greater than 1. This magnitude is calculated from the ratio of “no exo” to “exo”. For example the VMO results at 1.5ft would result in ratios of 1.83 (0-.25s), 1.61 (0-.75s), and 1.54 (0-1.25s). The ratio exceeding 1 is apparent in the other TA muscle at this height, however this is not the case for the SOL where their values include ratios of: SOL- 1.08 (0-.25s), 0.95 (0-.75s) and 0.89 (0-1.25s). TA- 1.83 (0-.25s) 1.62 (0-.75s) and 1.54 (0-1.25s). For all other cases in this experiment the SOL muscle and TA muscle data does not display ratios of greater or equal value to 1. The VMO on the hand produces this ratio across all the height levels.

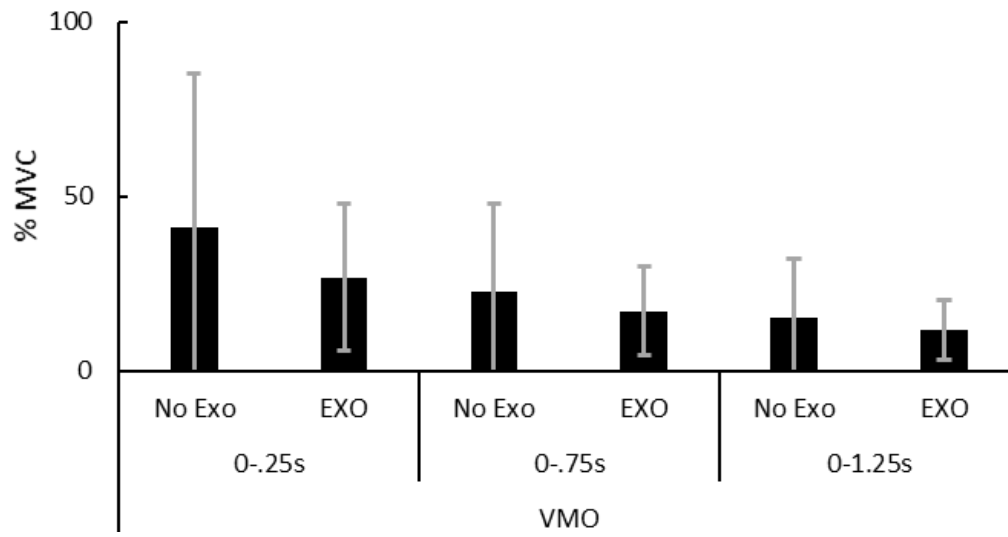


Figure 21 VMO 0.5ft

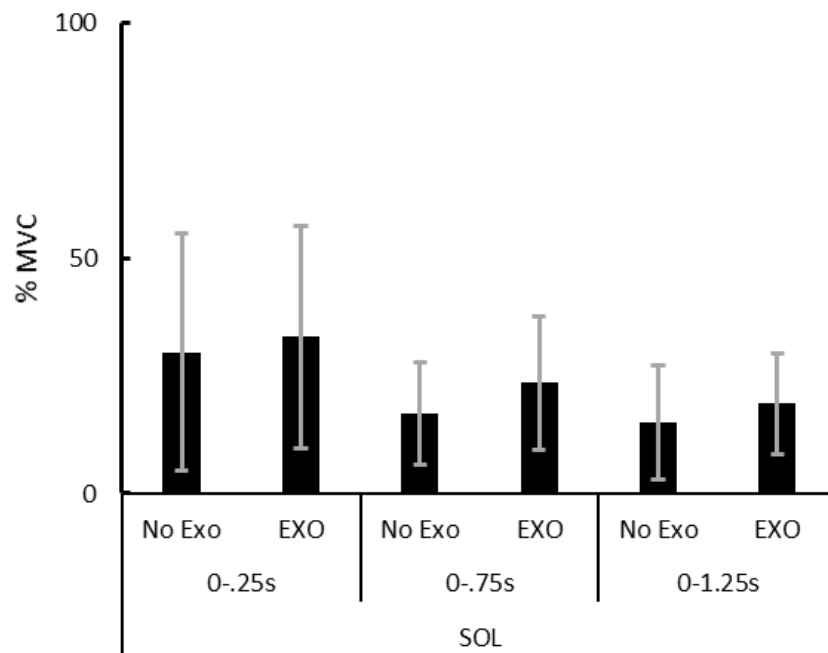


Figure 22 SOL 0.5ft

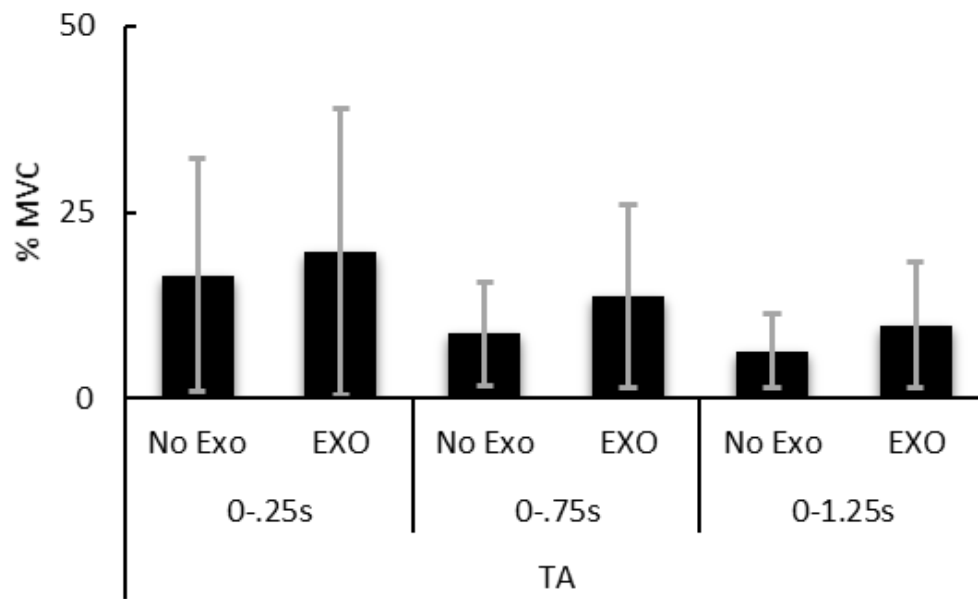


Figure 23 TA 0.5ft

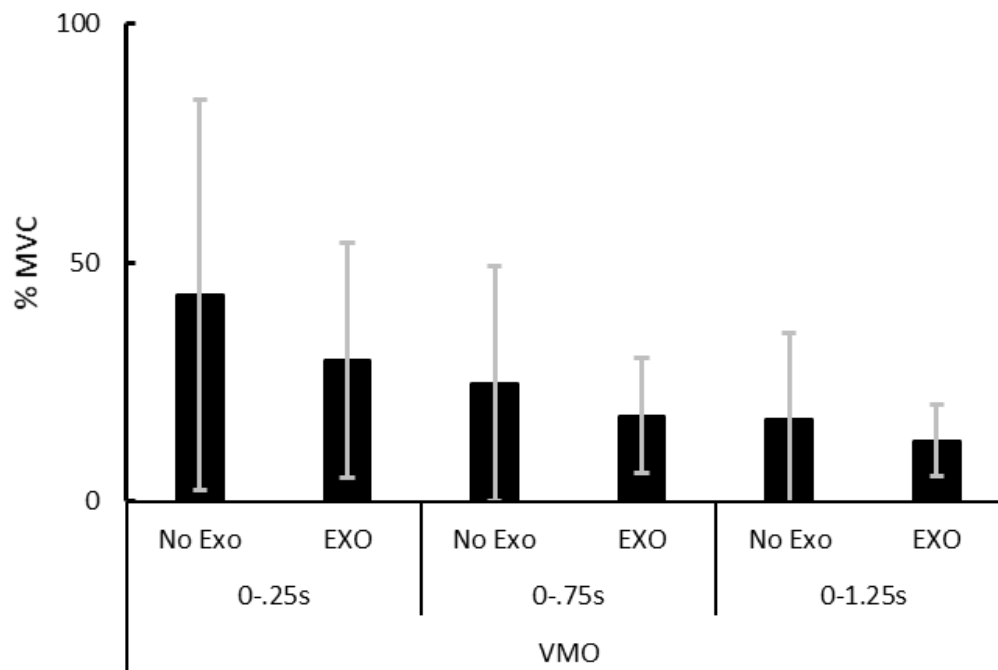


Figure 24 VMO 1.0ft

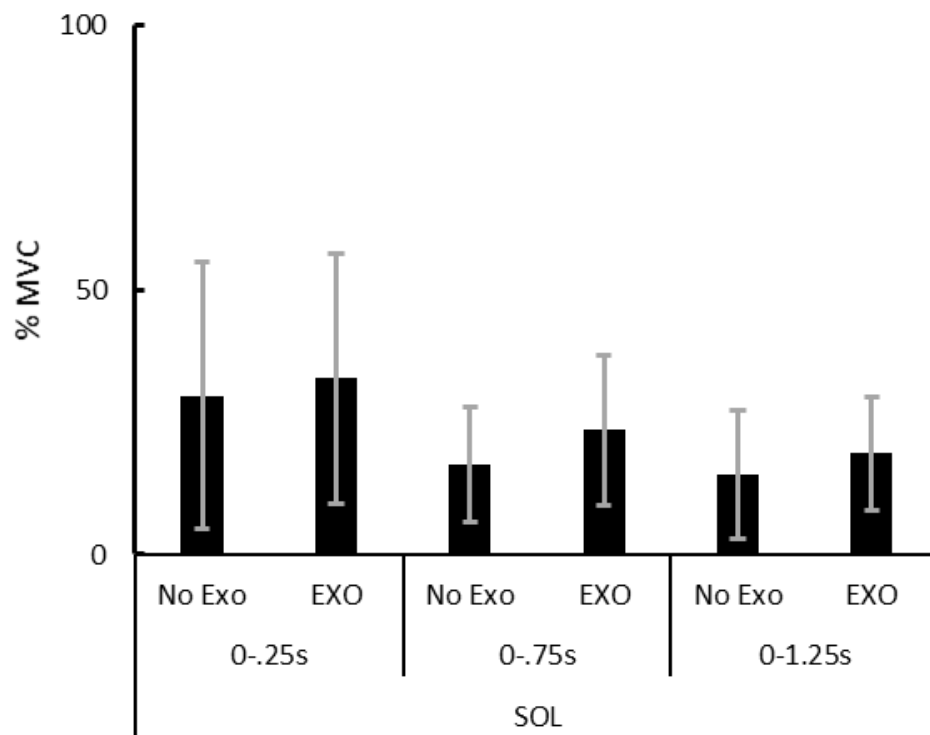


Figure 25 SOL 1.0ft

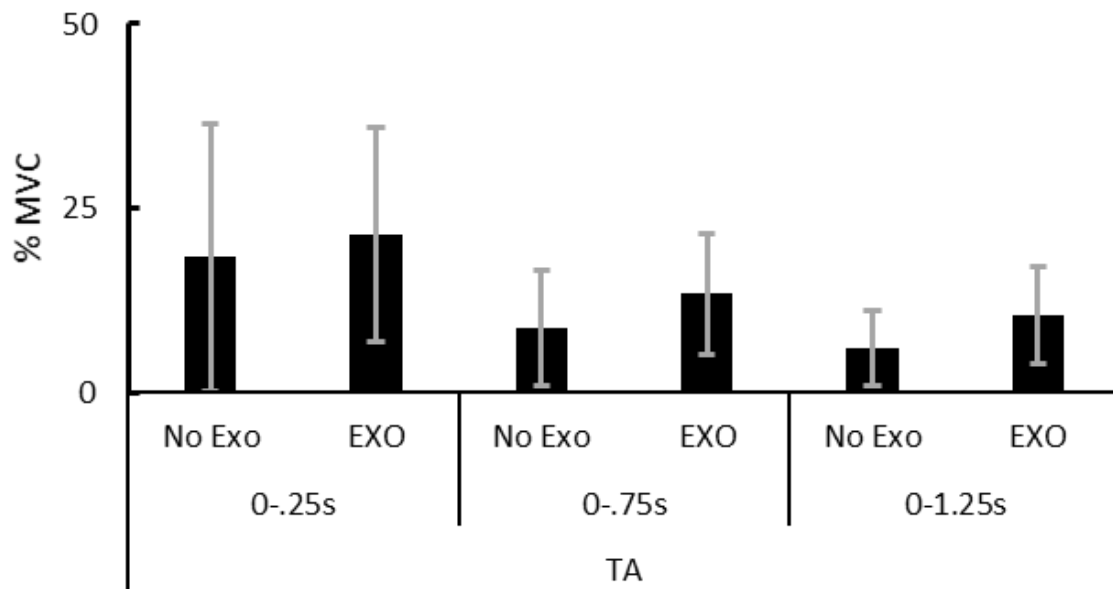


Figure 26 TA 1.0ft

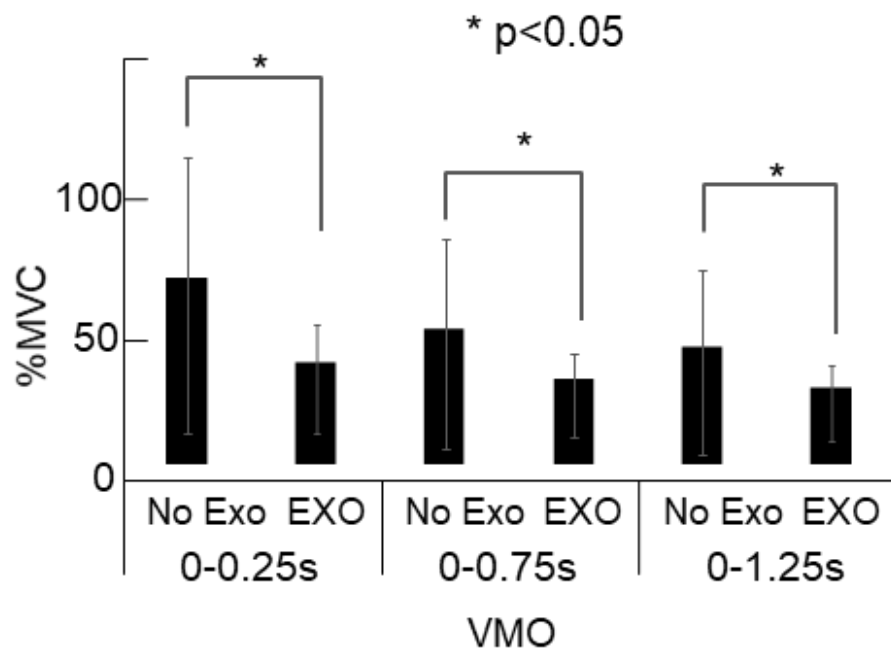


Figure 27 VMO 1.5ft

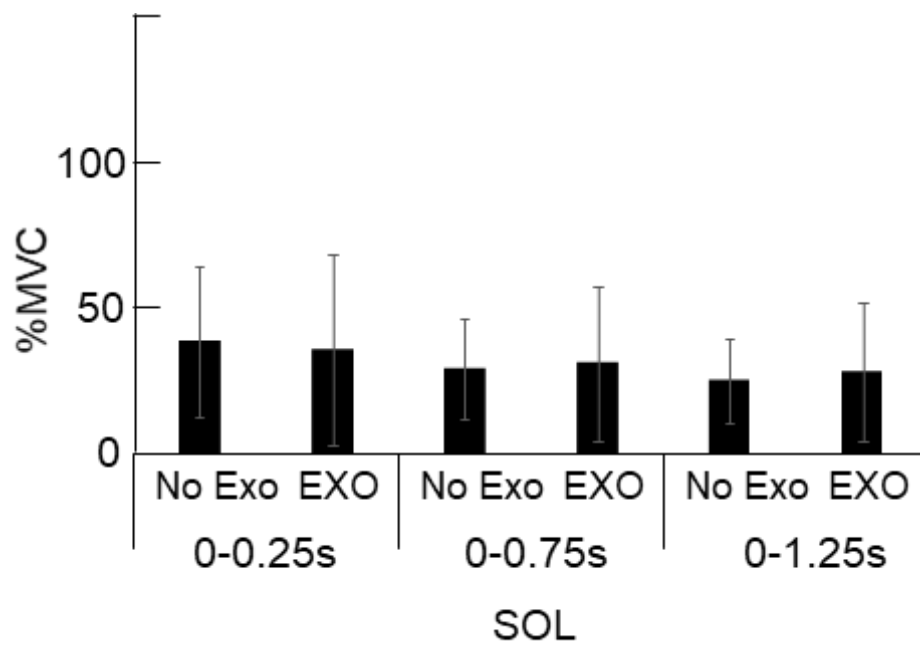


Figure 28 SOL 1.5ft

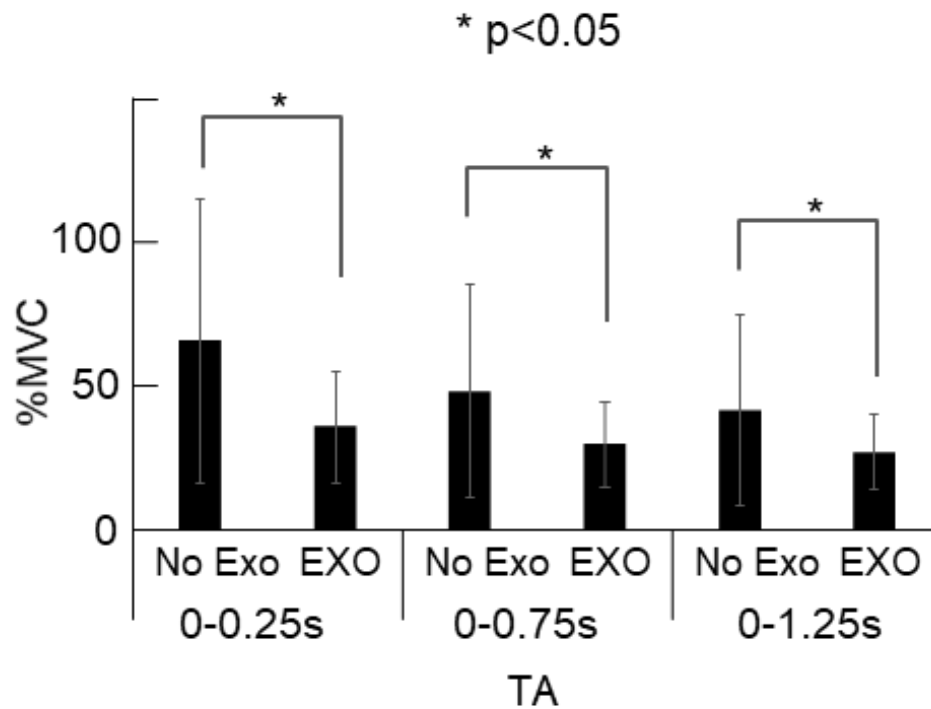


Figure 29 TA 1.5ft

The data that displays statistical significance are defined by the * symbol above the plots. Data that falls into that category includes Figure 29, TA muscle at 1.5ft jump height and Figure 27, VMO at 1.5ft. What is apparent is that unlike Figure 27 and 29, Figure 28 does not show statistical significance across all period for time analysis.

5.4 Discussion

Experimental data displaying the change in muscle activity showed expected results for shock absorbed performance when wearing the device—i.e., a dampening in the amount of muscle activity in the respective region for the VMO and TA. However, the expected declining trend was not observed at each time stamp for SOL. The current exoskeleton does not reduce muscle activities in all muscles in the leg. Muscles that contribute to

balancing after landing showed increased activities due to delayed response upon muscle excitement. Although not statistically tested, graphic displays of the data suggest that for all the subjects their VMO muscle experienced the greatest amount of activity when compared to the SOL and TA. The VMO muscle is larger than the other two muscles which does play into effect that amount of voltage received through the electrodes. The SOL muscle experienced the least amount of activity which may be due to the concept design which positioned the air cushion under the foot. The landing motion of the wearer does not fully excite the SOL muscle, because the landing places the user with primary pressure on the front of their foot.

The results of the TA muscle can be considered a reaction from dorsiflexion. Studies have proven that the dropping height significantly affects ankle dorsiflexion [14], this is characterized in Figure 28. The TA muscle data at a landing height of 1.5ft produces statistically significant data with a p-value $< .05$. The TA muscle at lower heights does not produce significant data due to the smaller amount of dorsiflexion.

The graphs that do not illustrate statistical significance is attributed to a number of factors; a large variation between the sampled data, outliers skewing the data, or too small of a confidence interval to include the given results. The p value chosen for this data set was .05, this value was chosen to not pigeon hole the data to a tight constraint. Also, a larger confidence interval would not represent the data accurately.

The lack in size of the soleus prevents it from producing a higher percentage in MVC when compared to the VMO and TA muscles. Other attributing factors to lower readings in the soleus is its slow response. The soleus late response is elicited during plantar flexion

[15]. The latency in soleus creates a delay in the activation which produces higher contraction values when wearing the exoskeleton. The average values of percentage of maximum voluntary contraction in the soleus do not exceed 45% of MVC.

In reviewing the results from EMG, understanding what makes EMG results greater or lesser is important. During contact with the ground immediately after impact the muscles excite. To state that the lower percentage of MVC is explicitly a protecting the muscles is inaccurate. For muscles to produce an EMG signal they need to contract on impact. EMG data can read lower in certain cases, however if protection in the admissible motion space and constrained motion space is the focus then contraction is needed to prevent a stiff landing. A stiff landing would create damage to bones and cartilage. What EMG data is displaying is how the muscles are reacting in the six varying scenarios and how the subject can rely on the muscles or device to secure the landing. Given the data from the statistically significant graphs Figure 29 and Figure 27, it is safe to conclude that at heights above 1.5ft the data in the VMO and TA muscle will be significant in that the exoskeleton will reduce the amount of muscle activity in these selected areas.

Chapter 6

Conclusion & Future Work

These results suggest that the concept design is a viable VMS—i.e., it should be explored further as a potential subsystem to enhance the jetpack. However, further research is needed to have the exoskeleton achieve full joint protection. Also, a larger number of subjects that includes a wider variation of ages and both sexes using the design in various situations could provide additional evidence that the exoskeleton is a proven system that should be considered along with the jetpack for military uses.

This study requires further understanding into effective protection as well satisfying the full mission requirement. This experiment focused on straight landing without the application of any weight that could resemble the use of payload or jet pack. Going forth with future designs, the implementation of an effective landing profile is beneficial to protecting the body and stability. Various landing practices could consist of staggered leg landings, spread leg landing, or bended knee landing. Each method can be studied to determine which best suits the wearer of the VMS with the expected payload weight. Understanding the best method of landing especially with a payload, reduces the risk injury in the legs, back, and other portions of the body. Another edition to the experiment is modifying how the jumps are performed, in terms of angle of attack. Realistically, during a mission the wearer may land in variation where they come in contact at an angle other than perpendicular to the ground. Testing the VMS across various terrains will benefit the device. Users will be using the device across numerous surfaces. It is imperative that the device is functional for majority surfaces.

Improving this research involves optimization of the system. Optimizing to where the user has on proper footwear that can assist in shock absorption and as well as mobility. Optimization also focuses on developing a supportive structure that can support the weight of the jet pack and prevent injury and limbs and other body parts.

Further study includes researching the tradeoffs between mobility and body protection. For the current prototype the point of emphasis was related to protection and mobility was not highly favorable. Based on other exo-systems, those that focus on mobility are less protective than devices that protect. A look into how the joints and muscles perform when the system provides more fluid locomotion would benefit the VMS. The integration of actuators and powered motion can benefit the system in that locomotion is enhanced, similar to those exoskeleton devices in chapter 2.

The study can focus on a specific demographic, considering the jetpack pilots are currently male ranging from the 6'0"-6'4" range. This research was not dependent upon subjects falling into this category. However, data will provide information to assist in understanding how the VMS performs with people of specific attributes. This in turn will hopefully reduce the large variation in subject results.

Appendix

Measurements

Measurement	Males		Females		Population Percentiles, 50/50 Males/Females		
	50th percentile	± 1S.D	50th percentile	± 1S.D.	5th	50th	95th
Standing							
1. Forward Functional Reach							
a. includes body depth	32.5	1.9	29.2	1.5	27.2	30.7	35.0
at shoulder	(31.2)	(2.2)	(28.1)	(1.7)	(25.7)	(29.5)	(34.1)
b. acromial process to	26.9	1.7	24.6	1.3	22.6	25.6	29.3
function pinch							
c. abdominal extension	(24.4)	(3.5)	(23.8)	(2.6)	(19.1)	(24.1)	(29.3)
to functional pinch							
2. Abdominal Extension Depth	9.2	0.8	8.2	0.8	7.1	8.7	10.2
3. Waist Height	41.9	2.1	40.0	2.9	37.4	40.9	44.7
	(41.3)	(2.1)	(38.8)	(2.2)	(35.8)	(39.9)	(44.5)
4. Tibial Height	17.9	1.1	16.5	0.9	15.3	17.2	19.4
5. Knuckle Height	29.7	1.6	28.0	1.6	25.9	28.8	31.9
6. Elbow Height	43.5	1.8	40.4	1.4	38.0	42.0	45.8
	(45.1)	(2.5)	(42.2)	(2.7)	(38.5)	(43.6)	(48.6)
7. Shoulder Height	56.6	2.4	51.9	2.7	48.4	54.4	59.7
	(57.6)	(3.1)	(56.3)	(2.6)	(49.8)	(55.3)	(61.6)
8. Eye Height	64.7	2.4	59.6	2.2	56.8	62.1	67.8
9. Stature	68.7	2.6	63.8	2.4	60.8	66.2	72.0
	(69.9)	(2.6)	(64.8)	(2.8)	(61.1)	(67.1)	(74.3)
10. Functional Overhead Reach	82.5	3.3	78.4	3.4	74.0	80.5	86.9
Seated							
11. Thigh Clearance Height	5.8	0.6	4.9	0.5	4.3	5.3	6.5
12. Elbow Rest Height	9.5	1.3	9.1	1.2	7.3	9.3	11.4
13. Midshoulder Height	24.5	1.2	22.8	1.0	21.4	23.6	26.1
14. Eye Height	31.0	1.4	29.0	1.2	27.4	29.9	32.8
15. Sitting Height, Normal	34.1	1.5	32.2	1.6	32.0	34.6	37.4
16. Functional Overhead Reach	50.6	3.3	47.2	2.6	43.6	48.7	54.8
17. Knee Height	21.3	1.1	20.1	1.9	18.7	20.7	22.7
18. Popliteal Height	17.2	1.0	16.2	0.7	15.1	16.6	18.4
19. Leg Length	41.4	1.9	39.6	1.7	37.3	40.5	43.9
20. Upper-Leg Length	23.4	1.1	22.6	1.0	21.1	23.0	24.9
21. Buttocks-to-Popliteal	19.2	1.0	18.9	1.2	17.2	19.1	20.9
Length							
22. Elbow-to-Fit Length	14.2	0.9	12.7	1.1	12.6	14.5	16.2
	(14.6)	(1.2)	(13.0)	(1.2)	(11.4)	(13.8)	(16.2)
23. Upper-Arm Length	14.5	0.7	13.4	0.4	12.9	13.8	15.5
	(14.6)	(1.0)	(13.3)	(0.8)	(12.1)	(13.8)	(16.0)
24. Shoulder Breadth	17.9	0.8	15.4	0.8	14.3	16.7	18.8

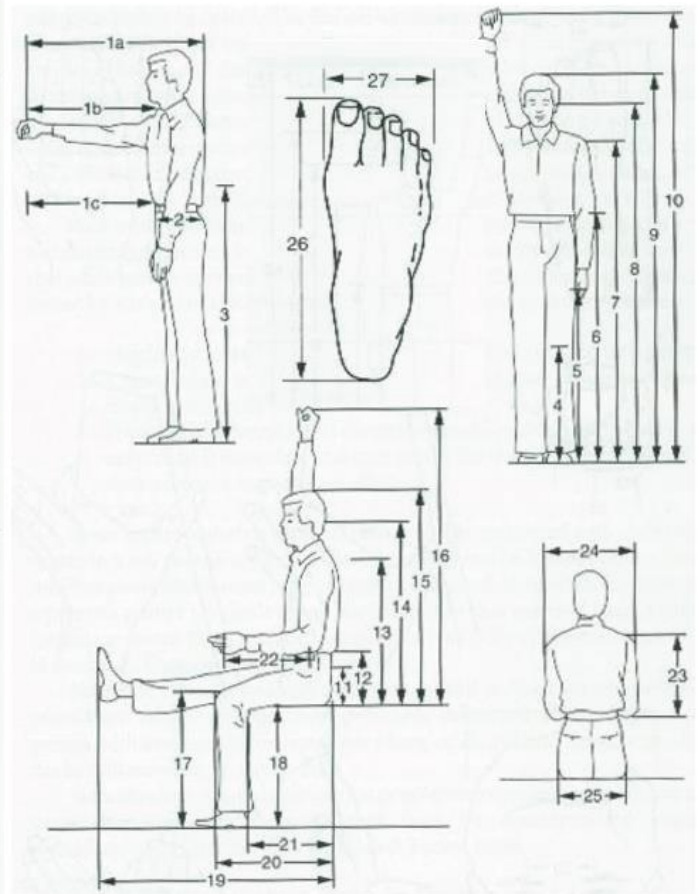


Figure A.1 Anthropometry Diagram

The following diagram, Figure A.1 was used to guide JetPack Aviation in collecting correct measurements for pilot to design VMS. Information provided is outlined in table A.1. Pilot dimensions were taken using English units and translated to SolidWorks to design VMS prototype.

Table A.1 Pilot Dimensions

Pilot	
Reference Number	Measurements (inches)
1a	30.5
1b	25
1c	21
2	9
3	46
4	20.6
5	34.9
6	48.5
7	64.2
8	70.5
9	74.5
10	89.25
11	7.5
12	11.5
13	27.8
14	34.3
15	38.9
16	51.1
17	23.4
18	20.4
19	44.75
20	25.4
21	21.1
22	15.2
23	19.2
24	18.5
25	15.8
26	11.5
27	4.75

References

1. A Brief History of Robotic Exoskeletons. (n.d.). Retrieved March 26, 2018, from <https://www.eduxo.com/resources/articles/exoskeleton-history/>
2. Blackburn, J. T., & Padua, D. A. (2008). Influence of trunk flexion on hip and knee joint kinematics during a controlled drop landing. *Clinical Biomechanics*, 23(3), 313-319. doi:10.1016/j.clinbiomech.2007.10.003
3. Chu, A., Kazerooni, H., & Zoss, A. (2005). On the Biomimetic Design of the Berkeley Lower Extremity Exoskeleton (BLEEX). *Proceedings of the 2005 IEEE International Conference on Robotics and Automation*, 4345-4352. doi:10.1109/robot.2005.1570789
4. H. Schiessel, R. Metzler, A. Blumen, and T. Nonnenmacher, "Generalized viscoelastic models: their fractional equations with solutions," *Journal of physics A: Mathematical and General*, vol. 28, no. 23, p. 6567, 1995.
5. Hopper, D. M., McNair, P., & Elliott, B. C. (1999). Landing in netball: Effects of taping and bracing the ankle. *British Journal of Sports Medicine*, 33(6), 409-413. doi:10.1136/bjsm.33.6.409
6. J. A. Buckwalter, D. D. Anderson, T. D. Brown, Y. Tochigi, and J. A. Martin, "The roles of mechanical stresses in the pathogenesis of osteoarthritis: implications for treatment of joint injuries," *Cartilage*, vol. 4, no. 4, pp. 286-294, 2013.
7. J. R. Steele, K. J. Mickle, and J. W. Whitting, "Preventing injuries associated with military static-line parachuting landings," in *The Mechanobiology and Mechanophysiology of Military-Related Injuries*. Springer, 2015, pp. 37-68.
8. Motor Vehicle Safety. (2017, September 21). Retrieved March 27, 2018, from <https://www.cdc.gov/motorvehiclesafety/seatbelts/index.html>
9. Soleus Muscle Origin, Function & Anatomy | Body Maps. (n.d.). Retrieved November 29, 2018, from <https://www.healthline.com/human-body-maps/soleus-muscle#1>
10. Tibialis Anterior Muscle - Anatomy Pictures and Information. (n.d.). Retrieved November 29, 2017, from http://www.innerbody.com/image_musc09/skel28.html#continued
11. Ueda, J., Turkseven, M., Kim, E., & Lowery, Q. (n.d.). Shock Absorbing Exoskeleton for Vertical Mobility System: Concept and Feasibility Study.

12. Umberger, B. R. (1998). Mechanics of the Vertical Jump and Two-Joint Muscles: Implications for Training. *Strength And Conditioning Journal*, 20(5), 70. doi:10.1519/1073-6840(1998)0202.3.co;2
13. Knapik, J. J., Graig, S. C., Hauret, K. G., & Jones, B. H. (n.d.). Risk Factors for Injuries During Military Parachuting. Retrieved April 20, 2018.
14. Niu, W., Wang, Y., He, Y., Fan, Y., & Zhao, Q. (2010). Biomechanical Gender Differences of the Ankle Joint During Simulated Half-Squat Parachute Landing. *Aviation, Space, and Environmental Medicine*, 81(8), 761-767. doi:10.3357/ase.2725.2010
15. Sakihara, K., Ihara, A., Takahashi, Y., Koreeda, S., Sakagami, A., Hirata, M., & Yorifuji, S. (2004). The late response in the soleus muscle evoked by transcranial magnetic stimulation at the foramen magnum level. *International Congress Series*, 1270, 146-148. doi:10.1016/j.ics.2004.05.085
16. Bressel, E., & Cronin, J. (2005). The Landing Phase of a Jump Strategies to Minimize Injuries. *Journal of Physical Education, Recreation & Dance*, 76(2), 30-35. doi:10.1080/07303084.2005.10607332
17. Withrow, T. J., Huston, L. J., Wojtys, E. M., & Ashton-Miller, J. A. (2006). The Relationship between Quadriceps Muscle Force, Knee Flexion, and Anterior Cruciate Ligament Strain in an in Vitro Simulated Jump Landing. *The American Journal of Sports Medicine*, 34(2), 269-274. doi:10.1177/0363546505280906
18. Mayman, D. (n.d.). JetPack Aviation. Retrieved February 4, 2018, from <http://www.jetpackaviation.com/>
19. Sanjeevi, R. (1982). A viscoelastic model for the mechanical properties of biological materials. *Journal of Biomechanics*, 15(2), 107-109. doi:10.1016/0021-9290(82)90042-2
20. Hidler, J., Nichols, D., Pelliccio, M., Brady, K., Campbell, D. D., Kahn, J. H., & Hornby, T. G. (2008). Multicenter Randomized Clinical Trial Evaluating the Effectiveness of the Lokomat in Subacute Stroke. *Neurorehabilitation and Neural Repair*, 23(1), 5-13. doi:10.1177/1545968308326632